A Two-Locus System with Strong Epistasis Underlies Rapid Parasite-Mediated Evolution of Host Resistance

Camille Ameline [iD],*[1] Yann Bourgeois [iD],[1,2] Felix Vögtli,[1] Eevi Savola [iD],[1,3] Jason Andras [iD],[1,4] Jan Engelstädter [iD],[5] and Dieter Ebert [iD][1]

[1]Department of Environmental Sciences, Zoology, University of Basel, Basel, Switzerland
[2]School of Biological Sciences, University of Portsmouth, Portsmouth, United Kingdom
[3]Institute of Evolutionary Biology, Ashworth Laboratories, University of Edinburgh, Edinburgh, United Kingdom
[4]Department of Biological Sciences, Clapp Laboratory, Mount Holyoke College, South Hadley, MA, USA
[5]School of Biological Sciences, The University of Queensland, Brisbane, QLD, Australia

*Corresponding author: E-mail: cameline8@gmail.com.
Associate editor: Deepa Agashe

Abstract

Parasites are a major evolutionary force, driving adaptive responses in host populations. Although the link between phenotypic response to parasite-mediated natural selection and the underlying genetic architecture often remains obscure, this link is crucial for understanding the evolution of resistance and predicting associated allele frequency changes in the population. To close this gap, we monitored the response to selection during epidemics of a virulent bacterial pathogen, *Pasteuria ramosa*, in a natural host population of *Daphnia magna*. Across two epidemics, we observed a strong increase in the proportion of resistant phenotypes as the epidemics progressed. Field and laboratory experiments confirmed that this increase in resistance was caused by selection from the local parasite. Using a genome-wide association study, we built a genetic model in which two genomic regions with dominance and epistasis control resistance polymorphism in the host. We verified this model by selfing host genotypes with different resistance phenotypes and scoring their F1 for segregation of resistance and associated genetic markers. Such epistatic effects with strong fitness consequences in host–parasite coevolution are believed to be crucial in the Red Queen model for the evolution of genetic recombination.

Key words: parasite-mediated selection, zooplankton, resistance, genetic architecture, epistasis, dominance, multi-locus genetics, *Daphnia magna*, *Pasteuria ramosa*.

Introduction

Darwinian evolution is a process in which the phenotypes that are best adapted to the current environment produce more offspring for the next generation. Genetic variants that code for these phenotypes are thus expected to increase in frequency in the population. Although this concept is fundamental in evolutionary biology, it remains difficult to connect the phenotype under selection with the underlying changes in the gene pool of natural populations (Ellegren and Sheldon 2008; Whitlock and Lotterhos 2015; Hoban et al. 2016). Although single-gene effects have been shown to explain the phenotype–genotype interplay in some naturally evolving populations (Daborn 2002; Cao et al. 2016; van't Hof et al. 2016), the genetic architecture underlying a phenotype is often complex. In addition, the way the environment influences the expression of a trait, and genotype × environment interactions may further obscure the link between phenotype and genotype. It is, thus, often impossible to predict genetic changes in a population that result from selection on specific phenotypes. Among the most potent drivers of evolutionary change in host populations are parasites; parasite-mediated selection can raise the frequency of resistant phenotypes rapidly (Schmid-Hempel 2011; Kurtz et al. 2016; Morgan and Koskella 2017; Koskella 2018) and is thought to contribute to many biological phenomena, such as biodiversity (Laine 2009), speciation (Schlesinger et al. 2014), and the maintenance of sexual recombination in the host (Lively 2010; Gibson et al. 2018).

To link patterns produced by parasite-mediated selection with evolutionary theory, we need to know the genetic architecture that underlies resistance; this includes the number of loci, their relative contribution to the phenotype, and the interaction between loci (epistasis) and alleles (dominance). In this way, we may be able to predict the outcome of selection, test theoretical models, and understand epidemiological dynamics (Hamilton 1980; Galvani 2003; Schmid-Hempel 2011). In a few cases, resistance to parasites has been found to be determined by single loci with strong effects, for example, in plants (Gómez-Gómez et al. 1999; Li and Cowling 2003; Li et al. 2017), invertebrates (Juneja et al. 2015; Xiao et al.

Open Access

2017), and vertebrates (Samson et al. 1996). However, the genetic architecture is often obscured by intrinsic complexity and confounding factors that may influence the phenotype. Resistance might be determined by multiple loci with qualitative or quantitative effects, present distinct dominance patterns, and display interactions with other genes or the environment. Indeed, multilocus genetic architecture of resistance can create more diversity, and is thus thought to be more common than single loci (Sasaki 2000; Tellier and Brown 2007; Wilfert and Schmid-Hempel 2008). Multilocus architecture was described in *Drosophila melanogaster*, for example, where resistance was found to be determined mostly by a few large-effect loci (Bangham et al. 2008; Magwire et al. 2012) and some additional small-effect loci (Cogni et al. 2016; Magalhães and Sucena 2016). Quantitative resistance has also been found in crops where it may be used as a pathogen control strategy (Pilet-Nayel et al. 2017). In the water flea *Daphnia magna*, resistance has been found to be quantitative to a microsporidian parasite, but qualitative to a bacterial pathogen (Routtu and Ebert 2015). Although resistance tends to be dominant (Hooker and Saxena 1971; Carton et al. 2005), resistant alleles have been found to be both dominant and recessive in plants (Gómez-Gómez et al. 1999; Li and Cowling 2003; Li et al. 2017) and invertebrates (Luijckx et al. 2012; Juneja et al. 2015; Xiao et al. 2017). Epistasis between resistance loci has also been found in diverse plants and animals (Kover and Caicedo 2001; Wilfert and Schmid-Hempel 2008; Jones et al. 2014; González et al. 2015; Metzger et al. 2016), emphasizing its crucial role in the evolution of resistance. The link between genetic architecture and natural selection for resistance remains weak, however, mainly limited to the theoretical extrapolation of results from laboratory experiments.

Dominance and epistasis describe the nonadditive interaction among alleles of the same or different loci, respectively, making them crucial for the evolutionary response to selection. Epistasis among resistance genes could contribute to the maintenance of genetic diversity by reducing fixation rates at individual loci, and is thus thought to be pervasive (Tellier and Brown 2007). In the Red Queen model for the evolution of sex, thus, epistasis among resistance loci helps maintain genetic diversity and recombination in the host (Hamilton 1980; Hamilton et al. 1990; Howard and Lively 1998; Salathé et al. 2008; Engelstädter and Bonhoeffer 2009; Kouyos et al. 2009). Important with regard to the role of epistasis for the evolution of host–parasite interactions is furthermore, that the interacting loci must be polymorphic within the same natural populations. However, the importance of genetic architecture for understanding the evolution of resistance stands in stark contrast to the limited amount of available data on natural populations (Alves et al. 2019). In this study, we investigate the evolution of resistance in a natural population of the planktonic crustacean *D. magna* as it experiences epidemics of the virulent bacterial pathogen *Pasteuria ramosa*. We link parasite-mediated selection to its associated allele frequency change by resolving the underlying genetic architecture of host resistance.

In recent years, water fleas of the genus *Daphnia* (Crustacea, Cladocera) and their microparasites have become one of the best understood systems for studying the evolution and ecology of host–parasite interactions (Ebert 2005; Vale et al. 2011; Izhar and Ben-Ami 2015; González-Tortuero et al. 2016; Strauss et al. 2017; Shocket et al. 2018; Turko et al. 2018; Rogalski and Duffy 2020). Parasite selection in natural *Daphnia* populations has been shown to alter the phenotypic distribution of resistance (Little and Ebert 1999; Decaestecker et al. 2007; Duffy and Sivars-Becker 2007; Duncan and Little 2007), and genetic mapping studies identified loci involved in host resistance (Luijckx et al. 2012, 2013; Routtu and Ebert 2015; Metzger et al. 2016; Bento et al. 2017, 2020) and parasite infectivity (Andras et al. 2020); however, because studies on host resistance largely involved crosses among populations, the results may not reflect genetic variation within populations. Genetic changes in natural host populations have been observed but so far it was not possible to link this change to parasite resistance loci (Mitchell et al. 2004; Duncan and Little 2007). Understanding the link between parasite-mediated selection on host resistance and the underlying genetic architecture would enable us to determine and predict the tempo and mode of evolution in natural populations and to link observed phenotypic changes to frequency changes of alleles under selection. This study provides such a phenotype–genotype link. We quantified the change in frequency of resistance phenotypes over time in a natural *D. magna* population and, through experiments, showed that the locally dominant, virulent parasite genotype of *P. ramosa* played a major role in the observed phenotypic changes. A genome-wide association study (GWAS) and genetic crosses revealed the underlying genetic architecture of resistance in our study population and provided a genetic model for inheritance of resistance. This genetic model comprises two resistance loci presenting distinct dominance patterns and strongly linked with epistasis. These results strongly support the Red Queen model of host–parasite coevolution and the maintenance of genetic recombination.

Results

Parasite-Mediated Selection Explains Phenotypic Dynamics

Monitoring

We monitored the Aegelsee *D. magna* population from fall 2010 to fall 2015, whereas the present study focuses on the 2014 and 2015 planktonic seasons. In this population, *D. magna* diapauses during winter as resting eggs, whereas the active season spans from early April to early October. Each summer, we observed a *P. ramosa* epidemic that typically started in early May, about a month after *Daphnia* emerged from diapause, and lasted throughout the summer (fig. 1A) with peak prevalence of 70–95%. *Pasteuria ramosa* infection in the host is characterized by gigantism, a reddish-brownish opaque coloration, and castration, that is, an empty brood pouch. *Pasteuria ramosa* is a virulent parasite, stripping the host of 80–90% of its residual reproductive success and
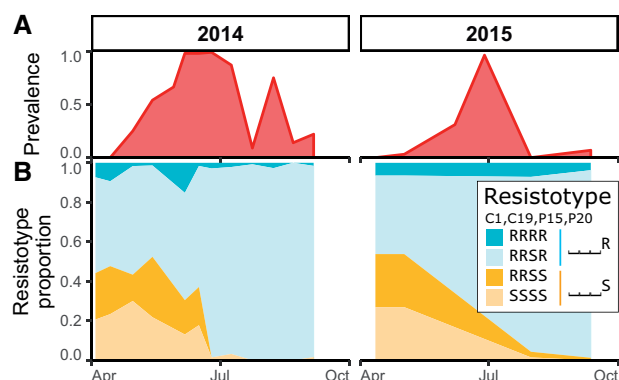
FIG. 1. Prevalence and resistotype dynamics observed in the Aegelsee *Daphnia magna* population. (*A*) *Pasteuria ramosa* prevalence across two summer epidemics. (*B*) Resistotype (resistance phenotype) frequencies across time (*n* = 60–100 *D. magna* clones from each sampling date in 2- to 3-week intervals). Resistotypes = resistance to *P. ramosa* C1, C19, P15, and P20, consecutively.

killing it after 6–10 weeks, at which point it releases millions of long-lasting spores into the environment (Ebert et al. 1996, 2016).

Animals sampled from the field were cloned, and their resistance phenotypes (resistotypes) were scored. *Daphnia magna* produces asexual clonal eggs which are used in the laboratory to produce clonal lines, a.k.a. genotypes. Individuals castrated by the parasite received an antibiotic treatment to allow clonal reproduction. Resistance to the bacteria is indicated when parasite spores are unable to attach to the gut wall of the host (Duneau et al. 2011; Luijckx et al. 2011). We thus defined host clone resistotypes according to the ability of parasite spores of given isolates to attach to the host gut wall or not. The host's overall resistotype is its combined resistotypes for the four *P. ramosa* isolates in the following order: C1, C19, P15, and P20, for example, a clone susceptible to all four isolates will have the SSSS resistotype. P20 had been isolated from our study population in May 2011; isolates C1, C19, and P15 had previously been established in the laboratory from other *D. magna* European populations. Overall, we found three predominant resistotypes: RRSR, RRSS, and SSSS, which together accounted for 95.1 ± 1.0% of all tested animals over the active season in 2014 (*n* = 995) and 2015 (*n* = 260). RRRR represented a much smaller proportion of the resistotypes (4.9 ± 1.0%) (fig. 1B). Excluding the resistotype data for *P. ramosa* isolate P15, for which over 95% of the hosts were susceptible, the study population was mainly composed of the three resistotypes: RR⌴R, RR⌴S, and SS⌴S. When one isolate was not considered, we used the placeholder "⌴" for that resistotype: for example, "RR⌴R resistotype." A few other resistotypes that were absent in the 2014 and 2015 samples were observed in other samples. Notably, the SR⌴S resistotype was found in 0.3% of hatched animals from *D. magna* resting eggs sampled during the winter 2014 diapause. The SR⌴R resistotype has never been found in the field samples but was found in the selfed offspring of the rare resistotype SR⌴S. Resistotypes RS⌴⌴ and SS⌴R were not observed in this population.

In 2011, we sampled a subset of infected animals (*n* = 113) to characterize *P. ramosa* diversity among infected hosts throughout the active season and found that the P20 genotype represented about 50% of the parasite diversity among infected hosts when the epidemics began. This proportion decreased to zero during the epidemic, as other *P. ramosa* genotypes took over (supplementary fig. S1, Supplementary Material online).

The temporal dynamics revealed an increase in animals resistant to P20 (RRSR and RRRR, in short: RR⌴R, or ⌴⌴⌴R) soon after the onset of the epidemics, whereas animals susceptible to P20 (RRSS and SSSS, or ⌴⌴⌴S) declined accordingly (fig. 1B) in both study years. Resistance to C1, C19, and P15 did not seem to play a strong role in the selection process during the epidemics. In the result described next, we tested the hypothesis that selection by *P. ramosa* isolate P20 is the main driver of natural resistotype dynamics in our study population during the early planktonic season. As a reminder, P20 has been isolated from a spring sample of the here-studied population.

Experimental and Field Infections

First, we tested the impact of the parasite on the different resistotypes to associate disease phenotype with resistotype. To do this, we obtained a sample of the spring cohort of the *D. magna* population by hatching resting eggs collected in February 2014. These animals represented, in total, 70 clones of the four most common resistotypes (RRSR, RRSS, SSSS, RRRR), with each clone replicated five times (*n* = 350). We exposed these clonal offspring to a mixture of *P. ramosa* spores that represented the diversity of the parasite population during the early phase of the epidemic. We then monitored the hosts for infection (looking for visible signs) and fecundity (counting the number of produced clutches). Sixteen animals died before we could test their infection status, resulting in a total sample size of *n* = 334. Individuals with resistotypes RRSS and SSSS (susceptible to P20) were infected far more frequently than RRSR and RRRR (resistant to P20) individuals (fig. 2A; null deviance = 461.3 on 333 df, residual deviance = 358.4 on 329 df, *P* < 0.001). The analysis also compared P20-susceptible and P20-resistant resistotypes, confirming the high susceptibility of the P20-susceptible animals (fig. 2A; null deviance = 461.3 on 333 df, residual deviance = 360.7 on 331 df, *P* < 0.001). Infected P20-susceptible individuals produced on an average about one less clutch before parasitic castration (*n* = 136, 1.83 ± 0.07 clutches) than did infected P20-resistant individuals (*n* = 19, 2.53 ± 0.3 clutches) (fig. 2B; null deviance = 76.9 on 154 df, residual deviance = 74.0 on 152 df, *P* = 0.023). Accordingly, the average time period until visible infection was shorter in P20-susceptible clones (15.7 ± 0.2 days) than in P20-resistant clones (19.4 ± 1 days) (fig. 2C; null deviance = 94.4 on 154 df, residual deviance = 85.1 on 152 df, *P* = 0.0018). These results clearly support the hypothesis that early season *P. ramosa* strains from the field select on the P20 resistotype.

In the following year, we looked at the relationship of disease phenotype and P20 resistotype only in the field by
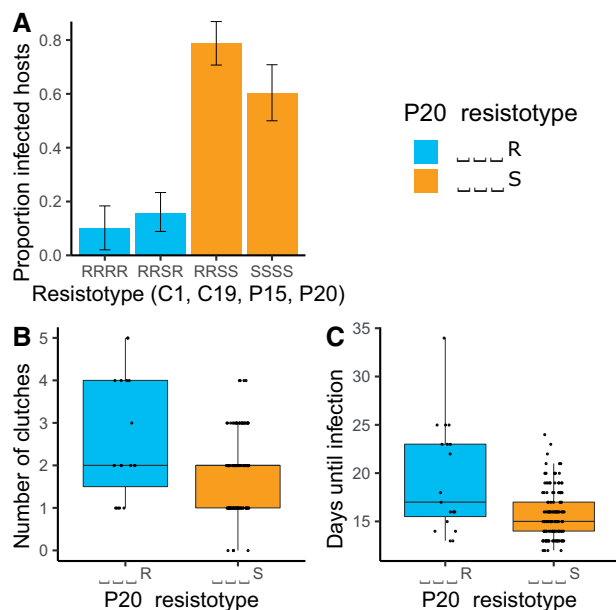
FIG. 2. Experimental infections of *Daphnia magna* with different resistotypes (resistance phenotype). Resistotypes RRSR, RRSS, SSSS ($n = 20$ clones for each), and RRRR ($n = 10$ clones) were infected with parasite spores from the early phase of the epidemic. Five repeats were performed for each clone (total $n = 334$). Controls ($n = 210$) remained uninfected and are not shown here. (A) Proportion of infected *D. magna* among the four resistotypes. (B) Number of clutches produced before parasitic castration in the infected P20-resistant (␣␣␣R) and susceptible (␣␣␣S) animals ($n = 115$). (C) Time before visible infection in P20-resistant and P20-susceptible individuals ($n = 115$).

FIG. 3. Fitted models of infection phenotypes in field-collected *Daphnia magna* relative to their body size at capture (*x* axis) and their resistance to P20 for two sampling dates in June 2015. (A) P20-susceptible (orange) animals have a higher likelihood to be infected than P20-resistant (blue) ones for any body size. (B) Infected P20-susceptible animals have a lower total fecundity than P20-resistant ones for any body size. Differences between the data are partially due to the difference in parasite prevalence on the two sampling dates (31% on June 7 and 96% on June 28).

measuring the parasite's impact on P20-resistant and P20-susceptible hosts. We collected animals in the field during the early half of the *P. ramosa* epidemic and raised them individually in the laboratory, recording their disease symptoms. We then cured infected animals with antibiotics, allowed them to produce clonal offspring, and determined their P20 resistotype. Our analysis revealed higher infection rates (size corrected) for P20-susceptible than for P20-resistant individuals in these natural conditions (fig. 3A; Fitted model: glm [Infected (1/0) ~ P20 resistotype + Body_size + Sampling_date], family = quasibinomial(), $n = 331$; null deviance $= 415.1$ on 330 df, residual deviance $= 209.1$ on 327 df, $P = 0.025$). Field-caught infected P20-susceptible individuals also produced, on an average, fewer offspring before parasitic castration than infected P20-resistant ones (fig. 3B; Fitted model: glm.nb [Fecundity ~ P20 resistotype + Body_size × Sampling_date], $n = 224$; null deviance $= 127.9$ on 223 df, residual deviance $= 92.9$ on 219 df, $P = 0.014$). In both models, the sampling date also had a significant effect. Parasite prevalence on the two sampling dates differed strongly (31% on June 7 and 96% on June 28, 2015). We observed on the first sampling date that larger individuals were more infected and consequently produced less offspring. This size difference is not visible anymore on the second sampling date, where almost all individuals were infected. The overall pattern in relation to the P20 resistotype remained the same, even though the difference in infection and fecundity between
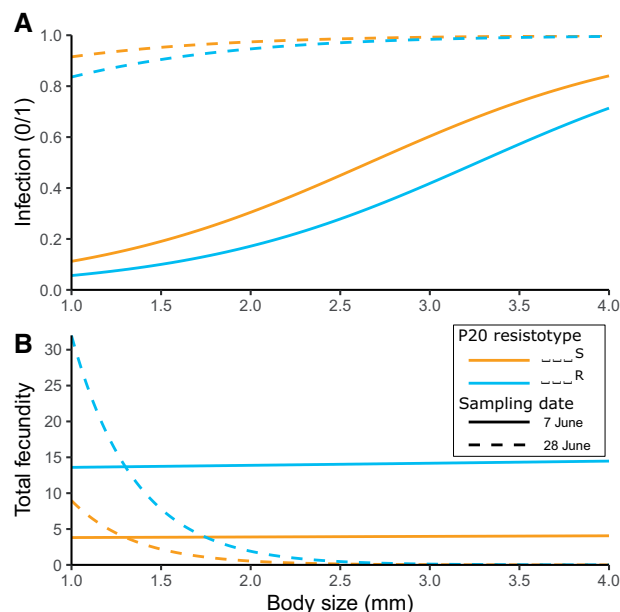
field-collected P20 resistotypes was less pronounced than in the controlled infection experiment (compare figs. 2 and 3). In summary, the results of the two experiments clearly support the hypothesis that early season *P. ramosa* from the field select on the P20 resistotype.

Linking Resistance Phenotypes to Genotypes

Excluding the P15 resistotype, which has very low variability because most animals are P15-susceptible, the study population was composed mainly of three resistotypes: RR␣R, RR␣S, and SS␣S. A supergene for resistance to C1 and C19 has been described in *D. magna* using QTL mapping (Routtu and Ebert 2015; Bento et al. 2017), and the genetic architecture of resistance at this so-called ABC-cluster, or *P. ramosa* resistance (PR) locus, has been further resolved using genetic crosses among host genotypes (Metzger et al. 2016). According to this genetic model, an SS␣␣ resistotype (susceptible to C1 and C19) has an "aabbcc" genotype (lower case letters indicate recessive alleles), whereas RS␣␣ individuals (resistant to C1 and susceptible to C19) are "A---cc" (upper case letters indicate dominant alleles and a dash "-" indicates alleles that do not influence the phenotype); SR␣␣ individuals are "aaB-cc," and RR␣␣ individuals are "----C-." In other words, allele A epistatically nullifies variation at the B locus, and allele C nullifies variation at the A and B loci (Metzger et al. 2016; Bento et al. 2017). See also supplementary figure S2, Supplementary Material online. Considering this genetic model, we assume that the recessive allele at the A locus is fixed in our study population ("aa" genotype)

and that the dominant allele at the B locus is very rare, as we never observed RS__ individuals and only found SR__ in very low proportions. In our study population, the SS__/ RR__ polymorphism can therefore be best described by the C-locus polymorphism, that is, genotypes "aabbcc" and "aabbC-", respectively, with C being the dominant allele for resistance. Given this, we assume, in the following sections, that variation at the C locus underlies the resistance polymorphism for C1 and C19.

Genomic Regions of Resistance to the Parasite

We sequenced the genomes of 16, 10, and 11 clones with resistotypes RR__R, RR__S, and SS__S, respectively and conducted a GWAS comparing five pairs of these resistotypes to identify candidates for resistance to C1, C19, and P20: (i) SS__ versus RR__, (ii) SS__S versus RR__S, (iii) ___S versus ___R, (iv) RR__S versus RR__R and (v) SS__S versus RR__R. Comparisons (i) and (ii) (variation at C1 and C19 resistotypes) revealed a strong signal on linkage group (LG) 3 (fig. 4A and B). This region encompasses the super gene described earlier by Routtu and Ebert (2015) and Bento et al. (2017), the so-called ABC-cluster, or PR locus. Comparisons (iii) and (iv) (variation at P20 resistotype) revealed a strong signal on LG 5 (fig. 4C and D), hereafter called the E-locus region. In the present host–parasite system, the D locus determines resistance to P15 and is not considered here (Bento et al. 2020). The E-locus region has not yet been associated with resistance, and no PR gene has been described on the same linkage group in D. magna. Finally, comparison (v) (variation at C1, C19, and P20 resistotypes) indicated a strong signal at both the ABC cluster and the E-locus region (fig. 4E). The genomic regions associated with resistotypes in our GWAS were not sharp peaks, but rather table-like blocks of associated SNPs (fig. 4). This structure was expected for the C locus, which is a known supergene—a large block of genome space with apparently little or no recombination that contains many genes (Bento et al. 2017). Figure 4 indicates that the same may be the case for the E-locus region, where the block of associated SNPs makes up nearly half of the linkage group. A few single SNPs also showed significant association in all the comparisons (fig. 4), but because of the strength of the observed pattern and because we expected a large region to be associated with resistance, we do not consider these single SNPs further.

The E-locus region encompassed 22 scaffolds and one contig on version 2.4 of the D. magna reference genome, with a cumulative length of more than 3 Mb (3,101,076 bp) (supplementary table S1, Supplementary Material online). We found 485 genes on all associated scaffolds. The strongest signals of association were found on scaffolds 2,167 and 2,560, which harbored 82 genes. Some of these genes were similar to genes identified in a previous study of the ABC cluster on LG 3 (Bento et al. 2017), with a glucosyltransferase found on scaffold 2,167. Three other sugar transferases (galactosyl-transferases) were identified, two of them on scaffold 2,560 (supplementary table S2, Supplementary Material online).

Genetic Model of Resistance Inheritance

Mean allele frequencies at associated SNPs showed that SS__ individuals (susceptible to C1 and C19) display a single allele at the C locus, whereas RR__ individuals display two distinct alleles at the C locus. This suggests that SS__ individuals are homozygous at the C locus, whereas RR__ individuals comprise homo- and heterozygotes. At the E locus, ___R individuals (resistant to P20) are presumably homozygous, whereas ___S individuals (susceptible to P20) comprise homo- and heterozygous individuals (fig. 4, right panel). These results indicate that resistance to C1 and C19 is governed by a dominant allele ("C-" genotype), as shown before (Metzger et al. 2016). In contrast, resistance to P20 is determined by a recessive allele ("ee" genotype), as was shown before for a different resistance locus (D locus, Bento et al. 2020). Screening individual genomes revealed that some SS__S individuals (susceptible to C1 and C19, and P20) present the "ee" genotype at the E locus (underlying P20 resistotype), although this genotype should confer resistance to P20. This was not observed in RR__S individuals (resistant to C1 and C19, but susceptible to P20) (supplementary table S3, Supplementary Material online), which we hypothesize to be explained by an epistatic relationship linking the C and the E loci. This epistasis confers P20 susceptibility to individuals susceptible to C1 and C19, that is, presenting the "cc" genotype, regardless of their genotype at the E locus. This genetic model is presented in figure 5 (without variation at the B locus, see below). In the present study, we mostly considered variation at the C and E loci, as they seem to play a major role in the diversity of resistotypes in our study population.

To test the genetic model derived from the GWAS, we investigated segregation of resistotypes among selfed offspring of D. magna genotypes with diverse resistotypes. Daphnia magna reproduces by cyclical parthenogenesis, in which asexual eggs produce clonal lines and sexual reproduction allows to perform genetic crosses. Our genetic model allowed us to predict the segregation of genotypes and phenotypes, which can then be compared with the observed segregation patterns among selfed offspring. From 24 host genotypes (F0 parent clones), we produced 24 groups of selfed F1 offspring. Twenty-two F0 clones included animals with all possible combinations of alleles at the C and E loci, whereas two F0s showed the rare variation at the B locus and variation at the E locus. Expected and observed resistotype frequencies are presented in tables 1 and 2 and detailed for each F1 group in supplementary tables S4–S15, Supplementary Material online. In the 22 F1 groups showing variation at the C and E loci, segregation of offspring followed the predictions of our genetic model (fig. 5), that is, we observed all expected resistotypes and saw no significant deviations from the expected frequencies based on the model. These data clearly support the genetic model for resistance at the C and E loci.

As described above, earlier research (Metzger et al. 2016; Bento et al. 2017) has shown that the dominant allele at the C locus interacts epistatically with the A and B loci (all are part of the ABC cluster), such that variation at the A and B loci
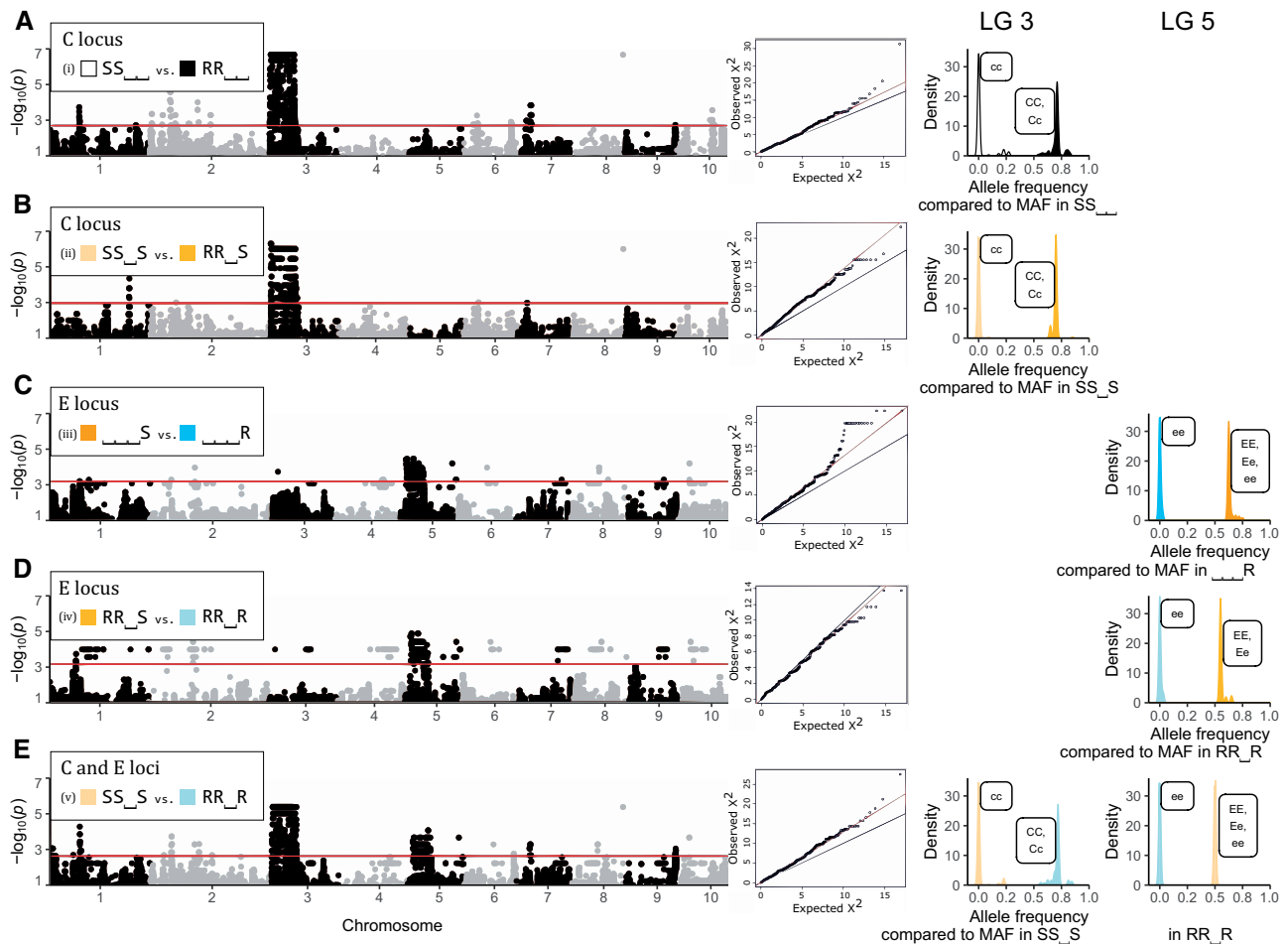
FIG. 4. GWAS analysis comparing the most common resistance phenotypes (resistotypes) in the Aegelsee *Daphnia magna* population. The resistotype depicts resistance (R) or susceptibility (S) to *Pasteuria ramosa* isolates C1, C19, P15, and P20. (i) SS⎵⎵ versus RR⎵⎵; (ii) SS⎵S versus RR⎵S; (iii) ⎵⎵⎵S versus ⎵⎵⎵R; (iv) RR⎵S versus RR⎵R, and (v) SS⎵S versus RR⎵R. Comparisons (i) and (ii) (variation at C1 and C19 resistotypes) revealed a strong signal on linkage group (LG) 3 corresponding to the C locus. Comparisons (iii) and (iv) (variation at P20 resistotype) revealed a strong signal on LG 5 corresponding to the E locus. Comparison (v) (variation at C1 and C19, and P20 resistotypes) revealed a strong signal on both regions. Left panel: Manhattan plots of relationships between different resistotype groups (showing only SNPs with $P_{corrected} < 0.01$). The x axis corresponds to SNP data mapped on the 2.4 *D. magna* reference genome (Routtu et al. 2014), representing only SNPs, not physical distance on the genome. Middle panel: Quantile-quantile plots of noncorrected P values excluding SNPs from linkage groups 3 and 5, since these scaffolds displayed an excess of strongly associated markers. Right panel: Comparison of allele frequencies between resistotype groups at the C and the E loci. Significant SNPs on LG 3 or LG 5 were used (SNPs with $P < P_{lim}/100$, with P_{lim} as defined in the Materials and Methods section, eq. 1). For each SNP, the allele with the minor allele frequency (MAF) within resistotype groups that presented only one allele at the C or the E locus (all homozygous individuals) was used for comparisons. Hence, the x axis represents allele frequency of the dominant allele within resistotype groups (considering total allele number, or chromosome number: 2n). Labels attached to peaks describe the inferred possible genotypes at the C or the E locus within resistotype groups. In comparisons at the C locus on LG 3, resistotype groups susceptible to C1 and C19 presented only one allele, that is, they contained only homozygous recessive individuals at the C locus (dominant allele frequency of zero). Resistotype groups resistant to C1 and C19 did contain the dominant allele (frequency between 0.5 and 1), showing that resistance is dominant at the C locus, as the resistant group contains heterozygous individuals. Similarly, in comparisons at the E locus on LG 5, resistotype groups resistant to P20 do not present the dominant allele (frequency of zero), whereas resistotype groups susceptible to P20 do, that is, contain heterozygous individuals (dominant allele frequency between 0.5 and 1). This shows that, in contrast with the C locus, susceptibility is dominant at the E locus. Screening individual genomes revealed that some SS⎵S individuals (susceptible to C1 and C19, and P20) presented the "ee" genotype at the E locus (resistance to P20), although susceptibility is dominant at the E locus. This was not observed in RR⎵S individuals (resistant to C1 and C19 but susceptible to P20) (supplementary table S3, Supplementary Material online). This observation can be explained by an epistatic relationship linking the C and the E loci. This epistasis confers susceptibility to P20 to individuals susceptible to C1 and C19, that is, presenting the "cc" genotype regardless of the genotype at the E locus. In contrast, with groups containing SS⎵S individuals, that is, comparisons (iii) and (iv), some SS⎵S individuals present the "ee" genotype at the E locus. In these groups, the frequency of the dominant allele can be lower than 0.5.
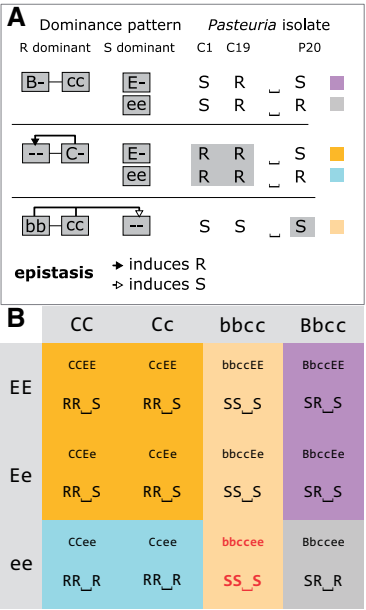
FIG. 5. Model for the genetic architecture of resistance to C1, C19, and P20 *Pasteuria ramosa* isolates in the Aegelsee *Daphnia magna* population as inferred from the GWAS analysis (fig. 4) and the genetic crosses (tables 1 and 2). (*A*) Schematic representation of the genetic model. Resistance to C1 and C19 is determined by the ABC cluster as described in Metzger et al. (2016), and the model is extended to include the newly discovered E locus. The dominant allele at the B locus induces resistance (R) to C19 and susceptibility (S) to C1. The dominant allele at the C locus confers resistance to both C1 and C19, regardless of the genotype at the B locus (epistasis). The newly discovered E locus contributes to determining resistance to P20. Resistance is dominant at the C locus (resistance to C1 and C19) but recessive at the E locus (resistance to P20). Homozygosity for the recessive allele at the B and C loci induces susceptibility to P20, regardless of the genotype at the E locus (epistasis). Hence epistasis can only be observed phenotypically in the "bbccee" genotype, which has the resistotype SS⌐S. Without epistasis, the "bbccee" genotype is expected to have the phenotype SS⌐R, a phenotype we never observed in the population or in our genetic crosses. (*B*) Multilocus genotypes and resistotypes at the B, C, and E loci. Resistotypes are grouped by background color. As the C allele epistatically nullifies the effect of the B locus, only combinations of the B and E loci are shown where the C locus is homozygous for the c allele. This model does not consider variation at the A locus, as the recessive allele at this locus is believed to be fixed in the Aegelsee *D. magna* population.

becomes neutral when a C allele is present. We assume that the a allele is fixed in the Aegelsee *D. magna* population, so that only variation at the B locus influences the C1 and C19 resistotypes in individuals with the "cc" genotype (see above). As variation at the B locus is very rare in our *D. magna* study population and could not be included in the GWAS analysis, we selfed two *D. magna* genotypes that presented the very rare SR⌐S resistotype, whose underlying genotype at the ABC cluster we expect to be "B-cc" (probably "Bbcc," considering the B allele is rare in the population). In the F1 offspring of the two F0 parents with the SR⌐S resistotype and the "Bbcc--" genotype, we observed SR⌐R individuals. We speculate that SR⌐R animals have the genotype "B-ccee,"

indicating that the epistatic relationship previously described between the C and the E loci ("cc" acts epistatically on the E locus) should also include the B locus. If this is the case, "bbcc" acts epistatically on the E locus (fig. 5). The two groups of selfed F1 offspring involving "Bb" heterozygotes showed a good fit between this expectation in the expanded model and the observed phenotypic segregation. We observed one SR⌐R offspring produced from a SR⌐S parent with the inferred "aaB-ccEE" genotype, which is not expected in our model (table 2B, lower panel), but typing mistakes cannot be fully ruled out.

Linking the Genomic Regions and the Genetic Model of Resistance

To test whether the segregation of the genomic regions, we discovered in the GWAS and the segregation of resistotypes in our crosses agreed with each other, we designed size-polymorphic markers in the genomic regions of the C and the E loci (two for each locus). We tested whether these markers cosegregated with the resistotypes as predicted by our genetic model. Of the four markers, DMPR1 (C locus) and DMPR3 (E locus) showed better linkage with their respective resistance loci (99.6% and 94.8% match, respectively) compared with DMPR2 (C locus) and DMPR4 (E locus) (91.4% and 69.4% match, respectively) (supplementary tables S16–S18, Supplementary Material online). These numbers reflect that our markers are close to the actual resistance loci, but that recombination between them is possible, leading to non-perfect association. We further based our scoring of resistance genotypes on the more predictive marker genotypes of DMPR1 and DMPR3. In 20 of 22 F1 groups representing all possible combinations of alleles at the C and E loci (table 1), the segregation of marker genotypes in the F1 offspring followed our genetic model predictions, that is, all expected genotypes were observed, with no statistically significant deviations from the expected frequencies. In two F1 groups from "CCEe" and "CcEe" F0 parents, the E-locus markers appeared not to be linked to the E locus (supplementary tables S5 and S8, Supplementary Material online). Based on the genotype markers results, we had assigned the "EE" genotype to the F0 parent and F1 offspring, but phenotypic segregation in the F1 offspring indicated the parent would have the "Ee" genotype. We speculate that recombination had uncoupled the genetic marker and the resistance loci in these two-parent genotypes. Together, these results show that the genomic regions found in the GWAS are indeed associated with the segregation of resistotype in the F1 selfed offspring, supporting our genetic model for the segregation of resistance (fig. 5).

Discussion

This present study aims to assess how annual epidemics by a parasitic bacterium, *P. ramosa*, influence resistance and the frequencies of the underlying genes in a natural host population of the crustacean *D. magna*. Over the course of epidemics in two consecutive years, we observed drastic changes in resistance phenotype (resistotype). Using experimental infections and fitness measurements on wild-caught

Table 1. Genetic Crosses of Resistance Phenotypes (resistotypes) from the Aegelsee *Daphnia magna* Population, Where Only the C and the E Loci Are Considered.

A

RR_S CcEe	CE	Ce	cE	ce
CE	RR_S	RR_S	RR_S	RR_S
Ce	RR_S	RR_R	RR_S	RR_R
cE	RR_S	RR_S	SS_S	SS_S
ce	RR_S	RR_R	SS_S	SS_S

B

F0 parent		Selfed F1 offspring							
				Proportion					
					Observed				
				Expected	Repeat (F1 groups from different parent clones)				C-M-H test on counts
Inferred genotype	Resistotype	Inferred genotype	Resistotype		a	b	c	d	
CCEE	RR_S	CCEE	RR_S	1	*n* = 43 1	*n* = 37 1			NA
CCEe	RR_S	CCE-	RR_S	0.75	*n* = 89 0.79	*n* = 31 0.74	*n* = 79 0.84		X^2=0.85, *df*=1, *p*=0.36
		CCee	RR_R	0.25	0.21	0.26	0.16		
CCee	RR_R	CCee	RR_R	1	*n* = 39 1	*n* = 42 1	*n* = 70 1	*n* = 79 1	NA
CcEE	RR_S	C-EE	RR_S	0.75	*n* = 19 0.74		*Fisher test on counts*		
		ccEE	SS_S	0.25	0.26				*p*=1
CcEe	RR_S	C-E-	RR_S	0.56	*n* = 48 0.47	*n* = 34 0.56	*n* = 64 0.65	*n* = 65 0.51	M^2=4.61, *df*=2, *p*=0.10
		cc--	SS_S	0.25	0.30	0.06	0.13	0.21	
		C-ee	RR_R	0.19	0.23	0.38	0.22	0.28	
Ccee	RR_R	C-ee	RR_R	0.75	*n* = 36 0.75	*n* = 49 0.80	*n*= 22 0.62		X^2=0.0062, *df*=1, *p*=0.94
		ccee	SS_S	0.25	0.25	0.20	0.38		
ccEE	SS_S	ccEE	SS_S	1	*n* = 87 1				NA
ccEe	SS_S	ccE-	SS_S	1	*n* = 84 1	*n* = 65 1			NA
ccee	SS_S	ccee	SS_S	1	*n* = 74 1	*n* = 35 1			NA

NOTE.—A, Punnett square for all possible gamete combinations according to our genetic model of resistance inheritance. The table shows the resistotypes (grouped by background color) from the 16 combinations of gametes from a double heterozygote for the C and the E loci. The bottom right cell (red font, italics) represents offspring individuals where the epistatic interaction between the C and the E loci is revealed (fig. 5); B, Results from selfing of *D. magna* clones. Resistotypes of F0 mothers and F1 offspring groups were obtained using the attachment test, and resistance genotypes of F0 parents at the C and E loci were inferred from their resistotypes and the segregation patterns of resistotypes in their F1 offspring. Expected resistotype proportions within F1 groups were calculated using the genetic model presented in the Punnett square and the R package "peas" (fig. 5 and supplementary doc. S1, Supplementary Material online). Detailed results and statistical analyses for each cross are presented in supplementary tables S4–S12 and S15, Supplementary Material online. Segregation of offspring is presented as proportions, although statistical tests were run on counts. One to four crosses using distinct mother clonal lines (repeats a to d) were conducted for each F0 mother resistance genotype at the C and E loci. No variation at the B locus was observed (all F0 mothers are inferred to have the "bb" genotype according to F1 resistotype segregation).

individuals, we showed that these changes in resistotype frequency were caused by a local parasite type common during the early phases of the epidemics. A GWAS and laboratory crosses enabled us to locate the resistance genes that responded to this selection and to uncover their mode of inheritance. We pinpointed the genetic architecture of resistance to two genomic regions with dominance and epistasis, thus bridging the gap between natural selection on phenotypes and the underlying genetics.

Parasite-Mediated Selection

Over the two consecutive years of this study, resistotype frequencies in the host population changed drastically during the parasite epidemics, but remained stable outside of the epidemics (fig. 1)—a pattern consistent with the host population being under strong selection for resistance to *P. ramosa*. The P20 *P. ramosa* isolate, collected during the early epidemic, turned out to be representative of the parasite population during the early part of the two epidemics studied here: Host genotypes characterized by their susceptibility to *P. ramosa* P20 drastically decreased in proportion during the epidemics and were much more susceptible to the local parasite than P20-resistant individuals in experimental infections (fig. 2A). Infected P20-susceptible genotypes also became infected earlier and produced fewer offspring than P20-resistant individuals (fig. 2B and C), revealing a stronger fitness impact of

Table 2. Genetic Crosses of Resistance Phenotypes (resistotypes) from the Aegelsee *Daphnia magna* Population Considering the B and the E Loci, with the C Locus Fixed for Genotype "cc."

A

SR_S BbccEe	BcE	Bce	bcE	bce
BcE	SR_S	SR_S	SR_S	SR_S
Bce	SR_S	SR_R	SR_S	SR_R
bcE	SR_S	SR_S	SS_S	SS_S
bce	SR_S	SR_R	SS_S	SS_S

B

F0 parent		Selfed F1 offspring				
Inferred genotype	Resistotype	Inferred genotype	Resistotype	Proportion		Fisher test on counts
				Expected	Observed	
					n = 37	
BbccEE	SR_S	B-ccEE	SR_S	0.75	0.74	
		bbccEE	SS_S	0.25	0.23	*p=1*
		B-ccee	SR_R	0.00	0.03	
					n = 38	
BbccEe	SR_S	B-ccE-	SR_S	0.56	0.56	
		bbcc--	SS_S	0.25	0.33	*p=0.58*
		B-ccee	SR_R	0.19	0.11	

NOTE.—A, Punnett square for all possible gamete combinations according to our genetic model of resistance inheritance. The table shows the resistotypes (grouped by background color) resulting from the 16 combinations of gametes from a double heterozygote for the B and the E loci. The bottom right cell (red font, italics) represents offspring individuals where the epistatic interaction between the B, the C, and the E loci is revealed (fig. 5); B, Results from selfing of *D. magna* clones. Resistotypes of F0 parents and F1 offspring were obtained using the attachment test, and resistance genotypes of F0 parents at the B, C, and E loci were inferred from their resistotypes and the segregation patterns of resistotypes in their F1 offspring. Expected resistotype proportions of F1 were calculated following the genetic model outlined in the Punnett square and using the R package "peas" (fig. 5 and supplementary doc. S2, Supplementary Material online). The detailed results and statistical analyses for each cross are presented in supplementary tables S13–S15, Supplementary Material online. Segregation of offspring is presented as proportions, although the statistical tests were run on counts.

infection by the local parasite. Field data confirmed this result, as wild-caught P20-susceptible individuals were infected more frequently and produced fewer offspring than infected P20-resistant individuals (fig. 3), again showing the higher virulence of the parasite in these P20-susceptible individuals. This effect of the parasite seemed less strong in field-collected animals than for those infected in the laboratory. Multiple factors may contribute to this, including differences among field and laboratory, and differences in the host and parasite populations from the two study years (2014 and 2015). Our findings reveal nevertheless a strong and rapid response to parasite-mediated selection on host resistotypes, that are characterized by their interaction with the P20 *P. ramosa* isolate, in the natural Aegelsee *D. magna* population.

In field samples, smaller individuals were found to be less infected than larger ones. This is not surprising, as older— hence bigger—animals have longer exposure to the parasite than younger animals. For a chronic disease like *P. ramosa* infections, it is expected that, with increasing size and age, prevalence will increase. These results are thus not in conflict with reports showing that younger—hence smaller *Daphnia*—were more susceptible to parasitic infections (Garbutt et al. 2014; Izhar and Ben-Ami 2015; Ben-Ami 2019). Differences in age-related susceptibility might, however, influence the shape of the body size—prevalence relationship observed in the field.

Although the parasite P20 was isolated during the early phase of the yearly epidemics, previous research also shows other parasite genotypes in the Aegelsee population (Andras and Ebert 2013) that, as we observed in an earlier year, become more common in infected hosts later in the epidemics (supplementary fig. S1, Supplementary Material online). We speculate that these later-season isolates may represent different parasite infectotypes (infection phenotypes). Consistent with this, we observed that animals resistant to P20 did, in fact, become infected, both in the field and in the laboratory (figs. 1–3), which cannot be explained with P20-infectotype parasites alone. The present study focuses on natural selection during the early part of the epidemics, which, as our data and data from other years shows, has a fairly consistent selection pattern (Ameline C, Vögtli F, Andras J, Engelstädter J, Ebert D, unpublished data), being mainly defined by a drastic increase in P20-resistant individuals from around 50% to almost 100% within a period of 2–3 months (fig. 1).

The composition of the resistotypes at the beginning of the two seasons (2014 and 2015) in which we monitored this system was strikingly similar, which is surprising given that selection increased resistance over the course of the summer 2014. Although answering this question is not part of the current study, there are a few tentative explanations for this observation. First, part of the yearly resting eggs yield, which form the basis of the new population in the following

spring, are produced as early as mid-June before selection has diminished some of the resistotypes. Second, epistasis and dominance can protect alleles from natural selection, thus slowing down the response to selection (Feldman et al. 1975; Otto 2009). Our study, as well as earlier studies on this system (Luijckx et al. 2012, 2013; Metzger et al. 2016), all indicate strong epistasis and dominance for resistance loci. Further studies are needed to understand how much resting egg production and the genetic architecture of resistance explain the slow response to selection observed across seasons in the Aegelsee *D. magna* population.

Genetic Architecture of Resistance

To understand the genetic architecture of resistance loci under selection in our study population, we combined a GWAS using *D. magna* genotypes with different resistotypes together with a series of genetic crosses. We found that the most diversity in host resistance to the bacteria is determined by variation at the C locus, situated in a previously described supergene, the PR locus containing the ABC cluster (Bento et al. 2017), and at a newly discovered locus on a different chromosome, the E locus (fig. 4). Taken alone and in the right genetic background, that is, when there is no epistatic relationship, each of these two loci show Mendelian segregation with resistance being dominant (C locus) or recessive (E locus) (fig. 4, right panel). The two loci interact epistatically with each other, resulting in a complex pattern of inheritance (fig. 5). Balancing selection is hypothesized to maintain diversity at resistance genes (Llaurens et al. 2017; Wittmann et al. 2017; Connallon and Chenoweth 2019), and these genes are often found to have different dominance patterns and epistatic interactions (Saavedra-Rodriguez et al. 2008; González et al. 2015; Conlon et al. 2018).

The E locus is situated on linkage group (LG) 5 (genome version 2.4: Routtu et al. 2014) and appears as a large region of 3.1 Mb (fig. 4). In this regard, the E locus is similar to the ABC cluster, a well-characterized, nonrecombining, and extremely divergent region on LG 3 (Bento et al. 2017). Nonrecombining genomic structures, that is, supergenes, are suggested to facilitate adaptation via association of advantageous alleles in host–parasite coevolution (Joron et al. 2011; Llaurens et al. 2017). Such large, diverse genomic regions are difficult to study because the absence of recombination hampers fine mapping (Bento et al. 2017). Therefore, we do not know where the actual resistance loci lie within the ABC- and E-loci regions. This may also explain why our genetic markers are not perfectly linked to the resistance loci (supplementary tables S17 and S18, Supplementary Material online). Supergenes may also harbor several resistance loci, thus variation at the C or the E locus could actually represent variation at several loci physically very close to each other. Within the E-locus region, we find four sugar transferases. Glycosylation genes are candidates to explain variation of resistance in this system (Bento et al. 2017; Bourgeois et al. 2017).

In the *D. magna*–*P. ramosa* system, the ABC cluster has been shown to play a major role in host resistance and the evolutionary dynamics of resistance (Routtu and Ebert 2015;

Bento et al. 2017; Bourgeois et al. 2017). Our results confirm the role of this cluster in a natural population and describe a new resistance region in the *D. magna* genome that is polymorphic in the Aegelsee population. Multilocus polymorphisms have been shown to underlie parasite resistance in host–parasite coevolution (Sasaki 2000; Tellier and Brown 2007; Cerqueira et al. 2017). In the Aegelsee *D. magna* population, there seems to be no variation at the A locus and little variation at the B locus. The observed variation at the B and C loci is consistent with the genetic model of resistance at the ABC cluster described in Metzger et al. (2016). In addition, resistance to *P. ramosa* isolate P15 (influenced by the D locus, Bento et al. 2020) remains fairly consistent, with the vast majority of animals being susceptible to P15 (fig. 1). Resistance to *P. ramosa* P21, also isolated from our study population, varies only toward the end of the summer epidemic (Ameline C, Vögtli F, Andras J, Engelstädter J, Ebert D, unpublished data). In summary, the ability to resist P20 plays a major role in the early epidemics and most resistotype diversity we measured in the Aegelsee *D. magna* population is well explained by genotypic variation at these loci. As we use more parasite isolates in further research, we might find other resistance regions in the *D. magna* genome. This is likely to be of importance in the later phase of the epidemics in the Aegelsee population.

Resistance segregation in *D. magna* is currently best explained by a genetic model where each locus contains just two alleles. This model was compiled by studies that used either mapping panels created from a few *D. magna* genotypes or, as here, host genotypes from one focal population. Additional resistance alleles may be revealed instead of new resistance regions if we test the genetic model on a larger panel of host and parasite genotypes.

We created 22 F1 offspring groups from the three common resistotypes in our study population. Segregation of resistance phenotypes and genotypes among the selfed F1 strongly supported the genetic model of resistance, consisting of the C and E loci, each with two alleles, and their epistatic interaction, produced by the GWAS (tables 1 and 2; supplementary tables S4–S15, Supplementary Material online). Two F1 offspring groups showed rare variation at the B locus, suggesting yet an additional epistatic interaction in this model besides the previously described role of the B locus for the *P. ramosa* C1 and C19 resistotypes. This consisted of the "bbcc" genotype that causes susceptibility to P20, irrespective of the genotype at the E locus (fig. 5). However, this modified model needs to be further investigated and verified with more genetic crosses.

Conclusion

In this study, we demonstrate rapid parasite-mediated selection in a natural plankton population. We find the genomic regions associated with resistance under selection and describe their mode of inheritance. This knowledge will allow us to conduct direct measurements of resistance allele frequency changes over time and to test theories on the dynamics of host and parasite coevolution, for example by

tracing genetic changes in the resting stages of *D. magna* derived from the layered sediments in ponds and lakes (Decaestecker et al. 2007). Pinpointing resistance loci can also be used to infer mechanisms of selection in the host with the molecular evolution tool box (Charlesworth 2006; Fijarczyk and Babik 2015; Hahn 2018). Our model of resistance consists of a few loci linked with epistasis and different dominance patterns, characteristics that have been shown to be relevant in coevolution, in particular when balancing selection maintains diversity at resistance genes (Tellier and Brown 2007; Engelstädter 2015; Conlon et al. 2018). The genomic regions we pinpoint can now be further studied, for example, by testing for genomic signatures for balancing selection (Charlesworth 2006; Ebert and Fields 2020). Hence, a precise knowledge of the genetic architecture of resistance opens the door to addressing wider evolutionary questions. For example, the Red Queen theory states that host–parasite interactions may explain the ubiquity of sex and recombination (Salathé et al. 2008).

Materials and Methods

Study Site
Our study site is the Aegelsee, a pond near Frauenfeld, Switzerland (code: CH-H for Hohliberg; coordinates: 47.557769 N, 8.862783 E, about 30,000 m² surface area) where *D. magna* is estimated to have a census population size over ten million individuals and an overwintering resting egg bank of about the same size. Every year from early October, the pond is used as a waste repository by a sugar factory: they progressively lower the water level from May to September and from October, warm ammoniacal condensation water is released into the pond, warming the water temporarily to 40–60 °C (Seefeldt and Ebert 2019) and killing all zooplankton, but not the resting eggs. In winter the pond usually freezes over, and in April, *Daphnia* and other invertebrates hatch from resting eggs. We sampled the pond in February 2014 and March 2015 and did not find *D. magna*, suggesting little or no overwintering. Besides *D. magna*, the plankton community includes *D. pulex*, *D. curvirostris* and a diverse array of other invertebrates, among them copepods, ostracods, rotifers, and corixids. The waste-water treatment prevents fish from invading the pond. The *D. magna* population experiences strong yearly epidemics of *P. ramosa*, reaching prevalence of 70–95%. Infections by other parasites were only rarely observed. The other *Daphnia* species in the pond were never observed to be infected by *P. ramosa*.

Temporal Monitoring
In 2014 and 2015, we sampled the host population every 2–3 weeks from early April to early October to study the impact of the pathogen epidemics. For each sampling date, we aimed to obtain about 100 cloned host lines (produced as iso-female lines). To achieve this, we randomly took about 200–300 female *D. magna* from the sample, placed them in 80-ml jars filled with ADaM (Artificial *Daphnia* Medium, Klüttgen et al. 1994, as modified by Ebert 1998) and let them reproduce asexually. Oversampling was necessary

during the hot summer months, as many animals would die for unknown reasons within 48 h under laboratory conditions. This mortality was, to the best of our knowledge, not disease related. Over the following 3 weeks, we screened animals for *P. ramosa* infections by checking for the typical signs of disease: gigantism, reddish-brownish opaque body coloration, and empty brood pouch. Infected animals that had not yet reproduced asexually were treated with tetracycline (50 mg l⁻¹) (an antibiotic which kills Gram-positive bacteria) until an asexual clutch was observed, usually after about 2 weeks. They were fed 25 million cells of the unicellular green algae *Scenedesmus* sp. three times a week, and the medium was renewed every 2 weeks. Feeding and fresh medium protocols were adapted according to the size and number of animals in a jar when necessary.

Resistotype Assessment: The Attachment Test
We assessed resistance phenotype (resistotype) for all cloned hosts using four *P. ramosa* isolates (C1, C19, P15, and P20). We isolated the parasite, P20, from our study population at the start of the epidemic on May 13, 2011 and subsequently passaged it three times through a susceptible *D. magna* host clone from the same population. The three other *P. ramosa* clones or isolates had been previously established in the laboratory: C1 (clone), originated from a *D. magna* population in Russia (Moscow), C19 (clone) from Germany (Gaarzerfeld) and P15 (isolate) from Belgium (Heverlee) (Luijckx et al. 2011; Bento et al. 2020). We used these three *P. ramosa* allopatric isolates in the present study to implement our working genetic model for resistance (Luijckx et al. 2012, 2013; Metzger et al. 2016). Parasite transmission stage (= spore) production in the laboratory followed the protocol by Luijckx et al. (2011).

The resistotypes of *D. magna* clones were assessed using a spore attachment test (Duneau et al. 2011). Bacterial spores attach to the foregut or the hindgut of susceptible host clones. Attachment is a prerequisite for subsequent infection. We call these genotypes susceptible, otherwise they are considered resistant. A genotype allowing attachment and penetration of the parasite into the host, may sometimes still resist infection, based on subsequent immune defense (Hall et al. 2019). To test for attachment, we exposed each individual *Daphnia* to 8,000 (C1, C19) or 10,000 (P15, P20) fluorescently labeled spores following the protocol of Duneau et al. (2011). We used higher spore doses for P15 and P20 because previous observations had shown that fewer of these isolate spores attach to the host esophagus, resulting in a weaker fluorescent signal. Three repeats were used for C1, C19, and P15, whereas six to nine repeats were used for P20. A clone was considered susceptible to the bacterial isolate when more than half of its replicates showed clear attachment. Its overall resistotype is the combination of its resistotypes to the four individual *P. ramosa* isolates in the following order: C1, C19, P15, and P20, for example, a clone susceptible to all four isolates would have resistotype SSSS. Since resistance to P15 had low variability in our study population, this isolate was only considered in the first experiment presented here and was otherwise represented with the placeholder "⌣", for example, "RR⌣R resistotype."

Experimental Infections of Resistotypes

As an initial assessment of the parasite's fitness impact on the host population, we conducted experimental infections on a representative sample of the spring 2014 host population. We collected surface sediment from five different points in the pond in February 2014, before onset of the natural hatching season and placed 100 *D. magna* ephippia from each replicate in 80-l containers with 30 l ADaM. The five containers were placed outdoors under direct sunlight and checked for hatchlings every 2 days. We recorded hatching dates and cloned hatchlings in the laboratory where we then scored their resistotypes. For the infection experiment, we used parasites collected from the ongoing epidemic in the pond. We collected three pools of 20 randomly chosen infected individuals during the first phase of the epidemic in early June 2014. These field-infected animals were kept in the laboratory under ad libitum feeding conditions. Shortly before their expected death, we pooled all 60 animals, homogenized them to produce a spore suspension, and froze it at −20 °C. A placebo suspension was produced from 60 homogenized uninfected *D. magna*. The parasite spore mixture was not passaged before we used it, so, in contrast to the isolates used for the attachment test, it represents a population sample of the parasite.

Among the four predominant resistotypes, we observed in the cloned cohort of spring hatchlings (SSSS, RRSS, RRSR, and RRRR), we used 20 clones each from the more common resistotypes SSSS, RRSS, and RRSR and ten of the less common resistotype RRRR for an infection experiment, due to limited availability. From each of these 70 clones, we produced five replicate lines, and these 350 lines were maintained individually in 80-ml jars. To reduce maternal effects before the experiment, we kept all lines for three generations in the same experimental conditions: 20 °C, 16:8 light:dark cycle, ADaM medium, and daily ad libitum feeding of 8 million *Scenedesmus* sp. cells per jar. The three generations were produced as follows: as soon as a female produced a clutch, she was discarded and the offspring were kept. When these offspring were mature, a single female was kept in the jar until she in turn produced a clutch. The medium was changed every 4 days or when the females released offspring. We exposed 2- to 3-day-old juveniles from all replicates to the parasite spore suspension by placing individual *D. magna* in 10 ml of medium with 10,000 spores. Additionally, three controls from the third-generation offspring were randomly taken from among the five replicates for each clone (n = 210) and were exposed to the equivalent volume of placebo suspension. Three days after exposure, the jars were filled to 80 ml. Medium was changed after ten days, and then every 4 days until the end of the experiment. Jars were monitored daily for 35 days. We recorded infection occurrence, clutch number, and time when visible signs of infection were observed. Controls did not get infected and produced offspring at regular intervals.

We tested both the effects of the full resistotype and of the P20 resistotype only on the three dependent variables: infection (binary: 1/0), clutch number (integer), and time of infection (continuous). Replicates were nested within clones, which were nested within resistotypes. We fitted general linear models using binomial data family type for infection and quasi-Poisson for clutch number and time to infection. For clutch size and time to infection, only data on infected individuals were used.

Infection Phenotypes of Field-Collected Hosts

As a second assessment of the impact of the local parasite on the host population, we measured fitness traits of animals caught during the epidemics. Because the infection experiment described above (carried out in the previous year) indicated that P20 played a strong role, we focused on this parasite isolate. On June 7 and 28, 2015, we collected large *D. magna* samples from our study site and measured body length, from the top of the head through the eye to the base of the tail spine. We kept all females (n = 331) individually under ad libitum feeding conditions, each in about 80 ml medium. We recorded clutches (time and size) and the onset time of disease symptoms over the following 3 weeks. After parasitic castration was evident, we cured animals with tetracycline. These data have also been reported in a paper describing the disease phenotype under natural conditions (Savola and Ebert 2019). The current data set is however smaller than the published data, as we report here only those animals for which we were able to score the resistotypes.

Using generalized linear models, we tested the effect of the P20 resistotype on infection and fecundity, taking body size into account. Sampling date was included as a fixed effect since there are only two sampling dates. Interaction terms were excluded from the model when not significant (P > 0.1). We fitted a general linear model using quasibinomial data family type for infection, and a negative binomial generalized linear model for total fecundity (R packages used: MASS: Venables and Ripley 2002, lme4: Bates et al. 2015).

Genome-Wide Association Study

Because our experiments revealed that resistance to P20 plays a major role in the disease dynamics in both laboratory experiments and the field, we used a genome-wide association approach to investigate the genetic architecture of resistance with 37 clones that presented the three most common resistotypes in our study population, excluding P15 resistotype (n = 16 RR◡R, 10 RR◡S, and 11 SS◡S). All 37 clones were derived directly from our study population (supplementary table S3, Supplementary Material online).

Whole-Genome DNA Extraction, Sequencing, and Bioinformatics

To remove microbial DNA, individuals were treated for 72 h with three antibiotics (streptomycin, tetracycline, ampicillin at a concentration of 50 mg l⁻¹ each in filtered water) and fed twice daily with 200 µl of a dextran bead solution (Sephadex G-25 Superfine by Sigma Aldrich: 20–50 µm diameter at a concentration of 5 g l⁻¹) to remove algae from the gut. DNA was extracted from 15 to 20 adult animals using an isopropanol precipitation protocol (QIAGEN DNeasy Blood

& Tissue Kit). Paired-end 125-cycle sequencing was performed on an Illumina HiSeq 2000.

$$P_{\text{corrected}} = P_{\chi 2}\left(\frac{\chi 2}{\lambda(\chi 2_{\text{LG}\neq 3\&5})}\right) \quad (1)$$

Raw reads were aligned using BWA MEM (Li and Durbin 2009) on the *D. magna* draft genome (v.2.4) and a genetic map (Routtu et al. 2014). BAM alignment files were then filtered for quality, and PCR duplicates were removed using PICARD tools (http://broadinstitute.github.io/picard/, last accessed December 2020). Variant calling was performed using freebayes (v. 0.9.15-1). VCF files were then filtered using VCFTOOLS v. 0.1.12b (Danecek et al. 2011) to include SNPs with a minimum quality of 20, a minimum genotype quality of 30, and a mean sequencing depth between $10\times$ and $50\times$. Only SNPs that passed filters in every clone sample were included in subsequent analyses, resulting in a data set of 510,087 SNPs. Association analyses were performed using the command "-assoc" in PLINK (Purcell et al. 2007), which compares allele counts between cases and controls and outputs a P value from a χ^2 test with one degree of freedom. Five pairwise comparisons were performed to identify possible candidates for resistance to C1, C19, and P20: (i) SS⌣⌣ versus RR⌣⌣, (ii) SS⌣S versus RR⌣S, (iii) ⌣⌣S versus ⌣⌣R, (iv) RR⌣S versus RR⌣R, and (v) SS⌣S versus RR⌣R. We corrected for the genomic inflation of P values (λ) that may have resulted from relatedness between samples using the R package GenABEL (Aulchenko et al. 2007). Lambda was calculated excluding SNPs from linkage groups 3 and 5, since these scaffolds displayed an excess of strongly associated markers. We divided raw χ^2 scores by λ to obtain corrected P values using R commands "pchisq" and "estlambda." For each SNP:

Histograms of corrected P values were examined to confirm their uniform distribution. We estimated the minimum false discovery rate incurred when a given P value was identified as significant (so-called q-value) from the set of corrected P values using the R package "qvalue" (Storey et al. 2015).

$$Q = q\text{value}(P_{\text{corrected}}) \quad (2)$$

The minimum significant threshold for a given association was then calculated as the maximum corrected P value with a q-value <5%.

$$P_{\text{lim}} = \max(P_{Q<0.05}) \quad (3)$$

The "gg.manhattan" function in R was used to display manhattan plots of the comparisons between different resistotypes (https://github.com/timknut/gg.manhattan/, last accessed December 2020). We used BEDTOOLS (v 2.25.0) to extract genes found in the associated candidate regions, using the 2011 annotation of the genome (available at: wfleabase.org, last accessed December 2020).

Assessment of Resistotype Segregation
The genetic model that resulted from the GWAS analysis allowed us to make predictions about the segregation of resistotypes in sexually reproducing *D. magna* lines. To test these predictions, we selfed *D. magna* clones with different resistotypes. Selfing is possible with *D. magna* because the same clonal line can produce sons (asexual production) as well as eggs by sexual production. The latter need fertilization by males. The resulting sexual eggs must undergo an obligatory resting phase before they can hatch (Ślusarczyk et al. 2019). The resistotypes of the selfed offspring (F1) were examined to assess whether their segregation matched expectations from the genetic model derived from the GWAS.

All clones used for the genetic crosses derived from the study population. We selfed five to ten *D. magna* clones of the three common resistotypes (RR⌣R, RR⌣S, and SS⌣S) and two clones of a rare resistotype (SR⌣S), following the protocol from Luijckx et al. (2012). Hatching of selfed offspring is not always successful, resulting in uneven sample sizes. We obtained between 19 and 89 selfed offspring from each of 22 parent clones (supplementary table S19, Supplementary Material online). Their resistotypes were assessed with the attachment test. Samples from each clonal line were stored at −20 °C for future DNA extraction and genotyping.

Predictions of Segregation Patterns
We compared the resistotype segregation patterns in the selfed offspring with predictions in our genetic model. To calculate proportions of expected phenotypes, we developed an R package called "peas" (https://github.com/JanEngelstaedter/peas, last accessed December 2020) that enables the user to predict distributions of offspring genotypes and phenotypes in complex genetic models with Mendelian inheritance (supplementary docs. S1 and S2, Supplementary Material online). We compared these predictions to the segregation patterns from our selfed offspring using the Cochran–Mantel–Haenszel (C–M–H) test for repeated tests of independence. The C–M–H test is applied either to 2 × 2 tables and outputs a chi-square statistic (χ^2) or to larger tables (generalized C–M–H test), where it outputs a M^2 statistic. When there was only one repeat per parent genotype, we used the Fisher's test. When there was only one category of expected and observed phenotype (i.e., no segregation), no test was possible, and expectation and observation showed a perfect match. Following each C–M–H test, assumption of homogeneity of the odds ratio across repeats was confirmed using a Breslow-Day test (R package DescTools: Signorell et al. 2018). However, this test can only be used with 2 × 2 tables. We ran a Fisher's test of independence on each comparison (expected vs. observed for each repeat, Bonferroni corrected) to detect differences in opposite directions across repeats, which would have resulted in a nonsignificant C–M–H test, but no such differences in direction were detected (see supplementary table S15, Supplementary Material online for detailed results of statistical analyses). Tests were run on counts, but for better illustration, we present here segregation of offspring as proportions.

Linking the Phenotype to the Genotype

We designed PCR-based diagnostic markers physically linked to the resistance loci that the GWAS identified (DMPR1 to 4 for "Daphnia magna–Pasteuria ramosa" markers, supplementary table S20, Supplementary Material online) and tested if these markers (and their corresponding resistance regions) are indeed associated with the resistotypes, by comparing expected and observed association between marker genotypes and resistotypes (supplementary tables S16–S18, Supplementary Material online). We then used these markers to confirm genotyping of the selfed parents.

DNA Extraction and PCR-Based Markers Analysis

DNA of parents and selfed offspring was extracted on 96-well PCR plates using a 10% Chelex bead solution (Bio-Rad) adapted from Walsh et al. (1991). First, individuals were crushed in the wells with 20 µl of deionized water using a customized rack of metallic pestles. We added 150 µl of 10% Chelex solution and 10 µl of proteinase K and incubated samples for 2 h at 55 °C followed by 10 min at 99 °C. Fragment amplification, genotyping, and allele scoring were done following the protocol described in Cabalzar et al. (2019) (see supplementary table S21, Supplementary Material online for PCR reaction details).

Statistical Software

Unless otherwise stated, all statistical analyses and graphics were performed using R software version 3.6.1 (R Core Team 2019). Graphics were edited in Inkscape v. 1.0.1 (https://inkscape.org/, last accessed December 2020). Mean values are presented with standard error: mean $\pm$ SE (Package RVAideMemoire v. 09-45-2, Hervé 2015). Packages used in R for package installation, data manipulation, and graphics are the following: package development, documentation, and installation: devtools v. 2.2.1 (Wickham, Hester, et al. 2019) and roxygen2 v. 6.1.1 (Wickham et al. 2018), data manipulation: dplyr v. 0.8.3 (Wickham, Francois, et al. 2019), tidyr v. 1.0.0 (Wickham and Henry 2019), tidyquant v. 0.5.8 (Dancho and Vaughan 2019), tidyverse v. 1.2.1 (Wickham 2017), xlsx v. 0.6.1 (Dragulescu and Arendt 2018), graphics: ggplot2 v. 3.3.0 (Wickham 2016), extrafont v. 0.17 (Chang 2014), scales v. 1.0.0 (Wickham 2018), cowplot v. 1.0.0 (Wilke 2019), gridExtra v. 2.3 (Auguie 2017), ggpubr v. 0.2.3 (Kassambara 2019), ggplotify v. 0.0.4 (Yu 2019), magick v. 2.2 (Ooms 2019), egg v. 0.4.5 (Auguie 2019), ggsci v. 2.9 (Xiao 2018), and png v. 0.1-7 (Urbanek 2013).

Supplementary Material

Supplementary data are available at Molecular Biology and Evolution online.

Author Contributions

D.E. and J.A. designed the overall study. F.V. and D.E. designed the infection experiment. F.V. conducted the infection experiment and analyzed the data. E.S. and D.E. designed the fitness measurements. E.S. conducted the fitness measurements and analyzed the data. Y.B. and D.E. designed the GWAS analysis. Y.B. conducted the GWAS analysis. C.A. and D.E. designed the crossings. C.A. conducted the crossings and analyzed the data. J.E. developed the "peas" R package. C.A. analyzed the data, wrote the manuscript, and designed the figures. All authors reviewed the manuscript.

Data Availability

The data underlying this article and analysis scripts are available in the Figshare Repository https://doi.org/10.6084/m9.figshare.13259828.v1. Raw sequence data from the GWAS analysis are deposited in the NCBI Bioproject PRJNA680821.

References

Alves JM, Carneiro M, Cheng JY, Lemos de Matos A, Rahman MM, Loog L, Campos PF, Wales N, Eriksson A, Manica A, et al. 2019. Parallel adaptation of rabbit populations to myxoma virus. Science 363(6433):1319–1326.

Andras JP, Ebert D. 2013. A novel approach to parasite population genetics: experimental infection reveals geographic differentiation, recombination and host-mediated population structure in Pasteuria ramosa, a bacterial parasite of Daphnia. Mol Ecol. 22(4):972–986.

Andras JP, Fields PD, Du Pasquier L, Fredericksen M, Ebert D. 2020. Genome-wide association analysis identifies a genetic basis of infectivity in a model bacterial pathogen. Mol Biol Evol.

Auguie B. 2017. gridExtra: miscellaneous functions for "Grid" graphics. Available from: https://CRAN.R-project.org/package=gridExtra. Last accessed on December 2020.

Auguie B. 2019. egg: extensions for "ggplot2": custom geom, custom themes, plot alignment, labelled panels, symmetric scales, and fixed panel size. Available from: https://CRAN.R-project.org/package=egg. Last accessed on December 2020.

Aulchenko YS, Ripke S, Isaacs A, van Duijn CM. 2007. GenABEL: an R library for genome-wide association analysis. Bioinformatics 23(10):1294–1296.

Bangham J, Knott SA, Kim K-W, Young RS, Jiggins FM. 2008. Genetic variation affecting host-parasite interactions: major-effect quantitative trait loci affect the transmission of sigma virus in Drosophila melanogaster. Mol Ecol. 17(17):3800–3807.

Bates D, Maechler M, Bolker B, Walker S. 2015. Fitting linear mixed-effects models using lme4. J Stat Softw. 67:1–48.

Ben-Ami F. 2019. Host age effects in invertebrates: epidemiological, ecological, and evolutionary implications. Trends Parasitol. 35(6):466–480.

Bento G, Fields PD, Duneau D, Ebert D. 2020. An alternative route of bacterial infection associated with a novel resistance locus in the *Daphnia–Pasteuria* host–parasite system. *Heredity* 125(4):173–183.

Bento G, Routtu J, Fields PD, Bourgeois Y, Du Pasquier L, Ebert D. 2017. The genetic basis of resistance and matching-allele interactions of a host-parasite system: the *Daphnia magna-Pasteuria ramosa* model. *PLoS Genet.* 13(2):e1006596.

Bourgeois Y, Roulin AC, Müller K, Ebert D. 2017. Parasitism drives host genome evolution: insights from the *Pasteuria ramosa–Daphnia magna* system. *Evolution* 71(4):1106–1113.

Cabalzar AP, Fields PD, Kato Y, Watanabe H, Ebert D. 2019. Parasite-mediated selection in a natural metapopulation of *Daphnia magna*. *Mol Ecol.* 28(21):4770–4785.

Cao C, Magwire MM, Bayer F, Jiggins FM. 2016. A polymorphism in the processing body component Ge-1 controls resistance to a naturally occurring Rhabdovirus in Drosophila. *PLoS Pathog.* 12:e1005387.

Carton Y, Nappi AJ, Poirie M. 2005. Genetics of anti-parasite resistance in invertebrates. *Dev. Comp. Immunol.* 29(1):9–32.

Cerqueira GC, Cheeseman IH, Schaffner SF, Nair S, McDew-White M, Phyo AP, Ashley EA, Melnikov A, Rogov P, Birren BW, et al. 2017. Longitudinal genomic surveillance of *Plasmodium falciparum* malaria parasites reveals complex genomic architecture of emerging artemisinin resistance. *Genome Biol.* 18(1):13.

Chang W. 2014. extrafont: tools for using fonts. Available from: https://CRAN.R-project.org/package=extrafont. Last accessed on December 2020.

Charlesworth D. 2006. Balancing selection and its effects on sequences in nearby genome regions. *PLoS Genet.* 2(4):e64.

Cogni R, Cao C, Day JP, Bridson C, Jiggins FM. 2016. The genetic architecture of resistance to virus infection in Drosophila. *Mol Ecol.* 25(20):5228–5241.

Conlon BH, Frey E, Rosenkranz P, Locke B, Moritz RFA, Routtu J. 2018. The role of epistatic interactions underpinning resistance to parasitic *Varroa* mites in haploid honey bee (*Apis mellifera*) drones. *J Evol Biol.* 31(6):801–809.

Connallon T, Chenoweth SF. 2019. Dominance reversals and the maintenance of genetic variation for fitness. *PLoS Biol.* 17(1):e3000118.

Daborn PJ. 2002. A single P450 allele associated with insecticide resistance in Drosophila. *Science* 297(5590):2253–2256.

Dancho M, Vaughan D. 2019. tidyquant: tidy quantitative financial analysis. Available from: https://CRAN.R-project.org/package=tidyquant. Last accessed on December 2020.

Danecek P, Auton A, Abecasis G, Albers CA, Banks E, DePristo MA, Handsaker RE, Lunter G, Marth GT, Sherry ST, et al. 2011. The variant call format and VCFtools. *Bioinformatics* 27(15):2156–2158.

Decaestecker E, Gaba S, Raeymaekers JAM, Stoks R, Van Kerckhoven L, Ebert D, De Meester L. 2007. Host–parasite 'Red Queen' dynamics archived in pond sediment. *Nature* 450(7171):870–873.

Dragulescu AA, Arendt C. 2018. xlsx: read, write, format Excel 2007 and Excel 97/2000/XP/2003 files. Available from: https://CRAN.R-project.org/package=xlsx. Last accessed on December 2020.

Duffy MA, Sivars-Becker L. 2007. Rapid evolution and ecological host-parasite dynamics. *Ecol Lett.* 10(1):44–53.

Duncan AB, Little TJ. 2007. Parasite-driven genetic change in a natural population of *Daphnia*. *Evolution* 61(4):796–803.

Duneau D, Luijckx P, Ben-Ami F, Laforsch C, Ebert D. 2011. Resolving the infection process reveals striking differences in the contribution of environment, genetics and phylogeny to host-parasite interactions. *BMC Biol.* 9(1):1–11.

Ebert D. 1998. Experimental evolution of parasites. *Science* 282(5393):1432–1436.

Ebert D. 2005. Ecology, epidemiology, and evolution of parasitism in *Daphnia*. Bethesda (MD): National Library of Medicine (US), National Center for Biotechnology Information.

Ebert D, Duneau D, Hall MD, Luijckx P, Andras JP, Du Pasquier L, Ben-Ami F. 2016. A population biology perspective on the stepwise infection process of the bacterial pathogen *Pasteuria ramosa* in *Daphnia*. *Adv Parasitol.* 91:265–310.

Ebert D, Fields PD. 2020. Host–parasite co-evolution and its genomic signature. *Nat Rev Genet.* 21:754–768.

Ebert D, Rainey P, Embley TM, Scholz D. 1996. Development, life cycle, ultrastructure and phylogenetic position of *Pasteuria ramosa* Metchnikoff 1888: rediscovery of an obligate endoparasite of *Daphnia magna* Straus. *Philos Trans R Soc B Biol Sci.* 351:1689–1701.

Ellegren H, Sheldon BC. 2008. Genetic basis of fitness differences in natural populations. *Nature* 452(7184):169–175.

Engelstädter J. 2015. Host-Parasite coevolutionary dynamics with generalized success/failure infection genetics. *Am Nat.* 185(5):E117–E129.

Engelstädter J, Bonhoeffer S. 2009. Red Queen dynamics with non-standard fitness interactions. *PLoS Comput Biol.* 5:e1000469.

Feldman MW, Lewontin RC, Frankin IR, Christiansen RB. 1975. Selection in complex genetic systems III. An effect of allele multiplicity with two loci. *Genetics* 79(2):333–347.

Fijarczyk A, Babik W. 2015. Detecting balancing selection in genomes: limits and prospects. *Mol Ecol.* 24(14):3529–3545.

Galvani AP. 2003. Epidemiology meets evolutionary ecology. *Trends Ecol Evol.* 18(3):132–139.

Garbutt JS, O'Donoghue AJP, McTaggart SJ, Wilson PJ, Little TJ. 2014. The development of pathogen resistance in *Daphnia magna*: implications for disease spread in age-structured populations. *J Exp Biol.* 217(21):3929–3934.

Gibson AK, Delph LF, Vergara D, Lively CM. 2018. Periodic, parasite-mediated selection for and against sex. *Am Nat.* 192(5):537–551.

Gómez-Gómez L, Felix G, Boller T. 1999. A single locus determines sensitivity to bacterial flagellin in *Arabidopsis thaliana*. *Plant J.* 18(3):277–284.

González AM, Yuste-Lisbona FJ, Rodiño AP, De Ron AM, Capel C, García-Alcázar M, Lozano R, Santalla M. 2015. Uncovering the genetic architecture of *Colletotrichum lindemuthianum* resistance through QTL mapping and epistatic interaction analysis in common bean. *Front Plant Sci.* 6:1–13.

González-Tortuero E, Rusek J, Turko P, Petrusek A, Maayan I, Piálek L, Tellenbach C, Gieler S, Spaak P, Wolinska J. 2016. *Daphnia* parasite dynamics across multiple *Caullerya* epidemics indicate selection against common parasite genotypes. *Zoology* 119(4):314–321.

Hahn MW. 2018. Molecular population genetics. New York: Oxford University Press.

Hall MD, Routtu J, Ebert D. 2019. Dissecting the genetic architecture of a stepwise infection process. *Mol Ecol.* 28:1–16.

Hamilton WD. 1980. Sex versus non-sex versus parasite. *Oikos* 35(2):282.

Hamilton WD, Axelrod R, Tanese R. 1990. Sexual reproduction as an adaptation to resist parasites (a review). *Proc Natl Acad Sci U S A.* 87(9):3566–3573.

Hervé M. 2015. RVAideMemoire: diverse basic statistical and graphical functions. Available from: http://CRAN.R-project.org/package=RVAideMemoire. Last accessed on December 2020.

Hoban S, Kelley JL, Lotterhos KE, Antolin MF, Bradburd G, Lowry DB, Poss ML, Reed LK, Storfer A, Whitlock MC. 2016. Finding the genomic basis of local adaptation: pitfalls, practical solutions, and future directions. *Am Nat.* 188(4):379–397.

Hooker AL, Saxena KMS. 1971. Genetics of disease resistance in plants. *Annu Rev Genet.* 5(1):407–424.

Howard RS, Lively CM. 1998. The maintenance of sex by parasitism and mutation accumulation under epistatic fitness functions. *Evolution* 52(2):604–610.

Izhar R, Ben-Ami F. 2015. Host age modulates parasite infectivity, virulence and reproduction. *J Anim Ecol.* 84(4):1018–1028.

Jones AG, Bürger R, Arnold SJ. 2014. Epistasis and natural selection shape the mutational architecture of complex traits. *Nat Commun.* 5:1–10.

Joron M, Frezal L, Jones RT, Chamberlain NL, Lee SF, Haag CR, Whibley A, Becuwe M, Baxter SW, Ferguson L, et al. 2011. Chromosomal rearrangements maintain a polymorphic supergene controlling butterfly mimicry. *Nature* 477(7363):203–206.

Juneja P, Ariani CV, Ho YS, Akorli J, Palmer WJ, Pain A, Jiggins FM. 2015. Exome and transcriptome sequencing of *Aedes aegypti* identifies a locus that confers resistance to *Brugia malayi* and alters the immune response. *PLoS Pathog.* 11(3):e1004765.

Kassambara A. 2019. ggpubr: "ggplot2" based publication ready plots. Available from: https://CRAN.R-project.org/package=ggpubr. Last accessed on December 2020.

Klüttgen B, Dülmer U, Engels M, Ratte HT. 1994. ADaM, an artificial freshwater for the culture of zooplankton. *Water Res.* 28(3):743–746.

Koskella B. 2018. Resistance gained, resistance lost: an explanation for host–parasite coexistence. *PLoS Biol.* 16(9):e3000013.

Kouyos RD, Salathé M, Otto SP, Bonhoeffer S. 2009. The role of epistasis on the evolution of recombination in host–parasite coevolution. *Theor Popul Biol.* 75(1):1–13.

Kover PX, Caicedo AL. 2001. The genetic architecture of disease resistance in plants and the maintenance of recombination by parasites. *Mol Ecol.* 10(1):1–16.

Kurtz J, Schulenburg H, Reusch TBH. 2016. Host-parasite coevolution-rapid reciprocal adaptation and its genetic basis. *Zoology* 119(4):241–243.

Laine A-L. 2009. Role of coevolution in generating biological diversity: spatially divergent selection trajectories. *J Exp Bot.* 60(11):2957–2970.

Li C, Cowling W. 2003. Identification of a single dominant allele for resistance to blackleg in *Brassica napus* "Surpass 400". *Plant Breed.* 122(6):485–488.

Li H, Durbin R. 2009. Fast and accurate short read alignment with Burrows-Wheeler transform. *Bioinformatics* 25(14):1754–1760.

Li W, Zhu Z, Chern M, Yin J, Yang C, Ran L, Cheng M, He M, Wang K, Wang J, et al. 2017. A natural allele of a transcription factor in rice confers broad-spectrum blast resistance. *Cell* 170(1):114–126.e15.

Little TJ, Ebert D. 1999. Associations between parasitism and host genotype in natural populations of *Daphnia* (Crustacea: Cladocera). *J Anim Ecol.* 68(1):134–149.

Lively CM. 2010. A review of Red Queen models for the persistence of obligate sexual reproduction. *J. Hered.* 101:S13–S20.

Llaurens V, Whibley A, Joron M. 2017. Genetic architecture and balancing selection: the life and death of differentiated variants. *Mol Ecol.* 26(9):2430–2448.

Luijckx P, Ben-Ami F, Mouton L, Du Pasquier L, Ebert D. 2011. Cloning of the unculturable parasite *Pasteuria ramosa* and its *Daphnia* host reveals extreme genotype-genotype interactions. *Ecol Lett.* 14(2):125–131.

Luijckx P, Fienberg H, Duneau D, Ebert D. 2012. Resistance to a bacterial parasite in the crustacean *Daphnia magna* shows Mendelian segregation with dominance. *Heredity* 108(5):547–551.

Luijckx P, Fienberg H, Duneau D, Ebert D. 2013. A matching-allele model explains host resistance to parasites. *Curr Biol.* 23(12):1085–1088.

Magalhães S, Sucena É. 2016. Genetics of host–parasite interactions: towards a comprehensive dissection of *Drosophila* resistance to viral infection. *Mol Ecol.* 25(20):4981–4983.

Magwire MM, Fabian DK, Schweyen H, Cao C, Longdon B, Bayer F, Jiggins FM. 2012. Genome-wide association studies reveal a simple genetic basis of resistance to naturally coevolving viruses in Drosophila melanogaster. *PLoS Genet.* 8:e1003057.

Metzger CMJA, Luijckx P, Bento G, Mariadassou M, Ebert D. 2016. The Red Queen lives: epistasis between linked resistance loci. *Evolution* 70(2):480–487.

Mitchell SE, Read AF, Little TJ. 2004. The effect of a pathogen epidemic on the genetic structure and reproductive strategy of the crustacean *Daphnia magna. Ecol Lett.* 7(9):848–858.

Morgan AD, Koskella B. 2017. Coevolution of host and pathogen (Second Edition). In: Tibayrenc M, editor. Genetics and evolution of infectious diseases. Elsevier. Sara Tenney. p. 115–140. Available from: http://linkinghub.elsevier.com/retrieve/pii/B9780127999425000068. Last accessed on December 2020.

Ooms J. 2019. magick: advanced graphics and image-processing in R. Available from: https://CRAN.R-project.org/package=magick. Last accessed on December 2020.

Otto SP. 2009. The evolutionary enigma of sex. *Am Nat.* 174(S1):S1–S14.

Pilet-Nayel M-L, Moury B, Caffier V, Montarry J, Kerlan M-C, Fournet S, Durel C-E, Delourme R. 2017. Quantitative resistance to plant pathogens in pyramiding strategies for durable crop protection. *Front Plant Sci.* 8:1838.

Purcell S, Neale B, Todd-Brown K, Thomas L, Ferreira MAR, Bender D, Maller J, Sklar P, de Bakker PIW, Daly MJ, et al. 2007. PLINK: a tool set for whole-genome association and population-based linkage analyses. *Am J Hum Genet.* 81(3):559–575.

R Core Team. 2019. R: a language and environment for statistical computing. Vienna (Austria): R Foundation for Statistical Computing. Available from: http://www.R-project.org. Last accessed on December 2020.

Rogalski MA, Duffy MA. 2020. Local adaptation of a parasite to solar radiation impacts disease transmission potential, spore yield, and host fecundity. *Evolution* 74:1856–1864.

Routtu J, Ebert D. 2015. Genetic architecture of resistance in *Daphnia* hosts against two species of host-specific parasites. *Heredity* 114(2):241–248.

Routtu J, Hall MD, Albere B, Beisel C, Bergeron RD, Chaturvedi A, Choi J-H, Colbourne J, De Meester L, Stephens MT, et al. 2014. An SNP-based second-generation genetic map of *Daphnia magna* and its application to QTL analysis of phenotypic traits. *BMC Genomics* 15(1):1033–1015.

Saavedra-Rodriguez K, Strode C, Flores Suarez A, Fernandez Salas I, Ranson H, Hemingway J, Black WC. 2008. Quantitative trait loci mapping of genome regions controlling permethrin resistance in the mosquito *Aedes aegypti. Genetics* 180(2):1137–1152.

Salathé M, Kouyos R, Bonhoeffer S. 2008. The state of affairs in the kingdom of the Red Queen. *Trends Ecol Evol.* 23(8):439–445.

Samson M, Libert F, Doranz BJ, Rucker J, Liesnard C, Farber C-M, Saragosti S, Lapouméroulie C, Cognaux J, Forceille C, et al. 1996. Resistance to HIV-1 infection in Caucasian individuals bearing mutant alleles of the CCR-5 chemokine receptor gene. *Nature* 382(6593):722–725.

Sasaki A. 2000. Host-parasite coevolution in a multilocus gene-for-gene system. *Proc R Soc Lond B.* 267(1458):2183–2188.

Savola E, Ebert D. 2019. Assessment of parasite virulence in a natural population of a planktonic crustacean. *BMC Ecol.* 19(1):14.

Schlesinger KJ, Stromberg SP, Carlson JM. 2014. Coevolutionary immune system dynamics driving pathogen speciation. *PLoS One* 9:e102821.

Schmid-Hempel P. 2011. Evolutionary parasitology. The integrated study of infections, immunology, ecology, and genetics. New York: Oxford University Press.

Seefeldt L, Ebert D. 2019. Temperature- versus precipitation-limitation shape local temperature tolerance in a Holarctic freshwater crustacean. *Proc R Soc B.* 286(1907):20190929.

Shocket MS, Vergara D, Sickbert AJ, Walsman JM, Strauss AT, Hite JL, Duffy MA, Cáceres CE, Hall SR. 2018. Parasite rearing and infection temperatures jointly influence disease transmission and shape seasonality of epidemics. *Ecology* 99(9):1975–1987.

Signorell A, et al. 2018. DescTools: tools for descriptive statistics. R package version 0.99.26.

Ślusarczyk M, Chlebicki W, Pijanowska J, Radzikowski J. 2019. The role of the refractory period in diapause length determination in a freshwater crustacean. *Sci Rep.* 9:11905.

Storey J, Bass A, Dabney A, Robinson D. 2015. qvalue: Q-value estimation for false discovery rate control. Available from: http://github.com/jdstorey/qvalue. Last accessed on December 2020.

Strauss AT, Hite JL, Shocket MS, Cáceres CE, Duffy MA, Hall SR. 2017. Rapid evolution rescues hosts from competition and disease but—despite a dilution effect—increases the density of infected hosts. *Proc R Soc B.* 284(1868):20171970.

Tellier A, Brown JKM. 2007. Polymorphism in multilocus host-parasite coevolutionary interactions. *Genetics* 177(3):1777–1790.

Turko P, Tellenbach C, Keller E, Tardent N, Keller B, Spaak P, Wolinska J. 2018. Parasites driving host diversity: incidence of

disease correlated with *Daphnia* clonal turnover. *Evolution* 72(3):619–629.

Urbanek S. 2013. png: read and write PNG images. Available from: https://CRAN.R-project.org/package=png. Last accessed on December 2020.

Vale PF, Wilson AJ, Best A, Boots M, Little TJ. 2011. Epidemiological, evolutionary, and coevolutionary implications of context-dependent parasitism. *Am Nat.* 177(4):510–521.

van't Hof AE, Campagne P, Rigden DJ, Yung CJ, Lingley J, Quail MA, Hall N, Darby AC, Saccheri IJ. 2016. The industrial melanism mutation in British peppered moths is a transposable element. *Nature* 534(7605):102–105.

Venables WN, Ripley BD. 2002. Modern applied statistics with S. 4th ed. New York: Springer.

Walsh PS, Metzger DA, Higuchi R. 1991. Chelex 100 as a medium for simple extraction of DNA for PCR-based typing from forensic material. *Biotechniques* 10(4):506–513.

Whitlock MC, Lotterhos KE. 2015. Reliable detection of loci responsible for local adaptation: inference of a null model through trimming the distribution of F_{ST}. *Am Nat.* 186(13):S24–S36.

Wickham H. 2016. ggplot2: elegant graphics for data analysis. New York: Springer-Verlag.

Wickham H. 2017. tidyverse: easily install and load the "Tidyverse." Available from: https://CRAN.R-project.org/package=tidyverse. Last accessed on December 2020.

Wickham H. 2018. scales: scale functions for visualization. Available from: https://CRAN.R-project.org/package=scales. Last accessed on December 2020.

Wickham H, Danenberg P, Eugster D. 2018. roxygen2: in-line documentation for R. Available from: https://CRAN.R-project.org/package=roxygen2. Last accessed on December 2020.

Wickham H, Francois R, Henry L, Müller K. 2019. dplyr: a grammar of data manipulation. Available from: https://CRAN.R-project.org/package=dplyr. Last accessed on December 2020.

Wickham H, Henry L. 2019. tidyr: tidy messy data. Available from: https://CRAN.R-project.org/package=tidyr. Last accessed on December 2020.

Wickham H, Hester J, Chang W. 2019. devtools: tools to make developing R packages easier. Available from: https://CRAN.R-project.org/package=devtools. Last accessed on December 2020.

Wilfert L, Schmid-Hempel P. 2008. The genetic architecture of susceptibility to parasites. *BMC Evol Biol.* 8(1):187.

Wilke CO. 2019. cowplot: streamlined plot theme and plot annotations for "ggplot2." Available from: https://CRAN.R-project.org/package=cowplot. Last accessed on December 2020.

Wittmann MJ, Bergland AO, Feldman MW, Schmidt PS, Petrov DA. 2017. Seasonally fluctuating selection can maintain polymorphism at many loci via segregation lift. *Proc Natl Acad Sci U S A.* 114(46):E9932–E9941.

Xiao N. 2018. ggsci: scientific journal and sci-fi themed color palettes for "ggplot2." Available from: https://CRAN.R-project.org/package=ggsci. Last accessed on December 2020.

Xiao Y, Dai Q, Hu R, Pacheco S, Yang Y, Liang G, Soberón M, Bravo A, Liu K, Wu K. 2017. A single point mutation resulting in cadherin mislocalization underpins resistance against *Bacillus thuringiensis* toxin in cotton bollworm. *J Biol Chem.* 292(7):2933–2943.

Yu G. 2019. ggplotify: convert plot to "grob" or "ggplot" object. Available from: https://CRAN.R-project.org/package=ggplotify.